

Isotopic Evidence for Variations in the Marine Calcium Cycle Over the Cenozoic

Christina L. De La Rocha^{1*} and Donald J. DePaolo^{1,2}

Significant variations in the isotopic composition of marine calcium have occurred over the last 80 million years. These variations reflect deviations in the balance between inputs of calcium to the ocean from weathering and outputs due to carbonate sedimentation, processes that are important in controlling the concentration of carbon dioxide in the atmosphere and, hence, global climate. The calcium isotopic ratio of paleo-seawater is an indicator of past changes in atmospheric carbon dioxide when coupled with determinations of paleo-pH.

Although there are extensive data on past variations in the isotopic ratios of such elements as Sr, C, and O in the oceans, there are few data that relate to major cation concentrations in ocean water of the past. Calcium (Ca^{2+}) is particularly interesting because of its relation to the rates of weathering of continental and seafloor silicate and carbonate rocks and the deposition of carbonate materials on the seafloor—processes that control atmospheric CO_2 concentrations (1–4) and thus strongly influence global temperature.

Although Ca^{2+} has a long residence time in the ocean ($\tau_{\text{Ca}} \approx 10^6$ years) (5), fluctuations in the seawater concentration of Ca^{2+} ($[\text{Ca}^{2+}]$) over geologic time are expected and have been inferred from geologic evidence (2, 3, 6–10). Even a small imbalance between Ca^{2+} inputs from weathering and outputs associated with carbonate deposition affects the seawater $[\text{Ca}^{2+}]$ (2, 3, 6–10). Similarly, such temporary inequalities between inputs and outputs should cause excursions in the isotopic composition of seawater Ca^{2+} ($\delta^{44}\text{Ca}$) (11).

The $\delta^{44}\text{Ca}$ of Ca^{2+} in present day seawater is uniform (Table 1) (12), as expected given the long residence time of Ca^{2+} relative to the ocean's mixing time of about 10^3 years (5). The $\delta^{44}\text{Ca}$ of modern seawater Ca^{2+} (Table 1) is $0.86 \pm 0.04\text{‰}$ (13). The $\delta^{44}\text{Ca}$ values of carbonate sediments of different age (Fig. 1) show systematic variation of the magnitude we expect, roughly coincident with major climatic events inferred from other records (14–19). We argue that these $\delta^{44}\text{Ca}$ data reflect variations in the $\delta^{44}\text{Ca}$ of paleo-seawater and indicate substantial variability in the global Ca^{2+} cycle.

The expected variability of $\delta^{44}\text{Ca}$ can be

estimated from a box model of the Ca^{2+} cycle. The source of Ca^{2+} to the oceans is the weathering of continental rocks and ocean-floor basalt (2, 3, 6–10, 20, 21), and the primary sink for marine Ca^{2+} is its biological fixation into carbonate sediments. The rate of change of $\delta^{44}\text{Ca}$ of the oceans ($= \delta_{\text{SW}}$) is given by

$$N_{\text{Ca}} \frac{d\delta_{\text{SW}}}{dt} = F_{\text{R}}(\delta_{\text{R}} - \delta_{\text{SW}}) + F_{\text{H}}(\delta_{\text{H}} - \delta_{\text{SW}}) - F_{\text{Sed}}\Delta_{\text{Sed}} \quad (1)$$

where N_{Ca} is the number of moles of Ca^{2+} in the oceans; F_{R} and F_{H} are the fluxes of Ca^{2+} from continental weathering and seafloor basalts, respectively; F_{Sed} is the rate of biological removal of Ca^{2+} into sediments (22); and Δ_{Sed} is the average $\delta^{44}\text{Ca}$ offset between biogenic carbonate and the seawater Ca^{2+} .

To evaluate the magnitude and variability of the fractionation associated with biological fixation of Ca^{2+} into carbonate (Δ_{Sed}), we measured $\delta^{44}\text{Ca}$ on foraminifera and coccolithophorids, the main carbonate-producing organisms in the ocean. The average $\delta^{44}\text{Ca}$ value of carbonate tests of the temperate intertidal foraminifera, *Elphidium ornatum*, collected over a 2-year interval from Bodega Bay, California (23), is offset from seawater Ca^{2+} by -1.2‰ , ranging from -1.1 to -1.5‰ . The fractionation of -1.1 to -1.5‰ for foraminifera tests appears to be applicable to biomineralization in a wide range of organisms. The coccolithophorid, *Emiliania huxleyi* (CCMP 1742), grown in the laboratory at 16°C , produced calcium carbonate with a $\delta^{44}\text{Ca}$ of -0.32 ± 0.16 and $-0.39 \pm 0.12\text{‰}$, 1.3‰ lower than the $\delta^{44}\text{Ca}$ of $+0.98 \pm 0.20\text{‰}$ of the Ca^{2+} present in the seawater growth medium (24). A fractionation of -1.2 to -1.5‰ has also been documented between dietary Ca^{2+} and bone Ca^{2+} in animals (25). From these data, our estimate for the global mean value of Δ_{Sed} is -1.3‰ (26).

Variations in Δ_{Sed} with temperature

would complicate reconstruction of δ_{SW} from carbonate sediments. Over the small temperature range investigated (Fig. 2), there is a weak correlation between growth temperature and $\delta^{44}\text{Ca}$ ($r^2 = 0.45$), the slope of which is not significantly different than 0 ($P = 0.05$). Previous observations also suggest that fractionation varies by less than 0.4‰ in foraminifera over a wide range of growth temperature (12). Hence, we conclude that the temperature dependence of the fractionation factor is small enough that the global average value is well defined.

The $\delta^{44}\text{Ca}$ of the modern weathering fluxes can be estimated from measurements of rocks, river waters, and marine carbonates. Silicate rocks have a $\delta^{44}\text{Ca}$ of $+0.3$ to -0.3‰ with an average close to 0‰ (27). The $\delta^{44}\text{Ca}$ values for six large rivers (12) (normalized to the standard we are using) (28) are slightly lower than this, yielding an average $\delta^{44}\text{Ca}$ of $-0.3 \pm 0.2\text{‰}$. By material balance, the long-term weathering flux must have $\delta^{44}\text{Ca}$ equal to that of the long-term average of δ_{sed} , which we calculate from the data of Fig. 1A to be -0.44‰ . Consequently, the present data suggest that the carbonate weathering flux may have a lower $\delta^{44}\text{Ca}$ than the silicate flux and that the weathering flux is dominated by Ca^{2+} derived from the weathering of old carbonate rocks (29).

For a steady-state ocean, where δ_{SW} and N_{Ca} are both unchanging with time, Eq. 1 reduces to

$$\delta_{\text{SW}} = \delta_{\text{W}} - \Delta_{\text{Sed}} \quad (2)$$

where δ_{W} is the isotopic composition of the combined continental and seafloor basalt weathering fluxes to the ocean. On the basis

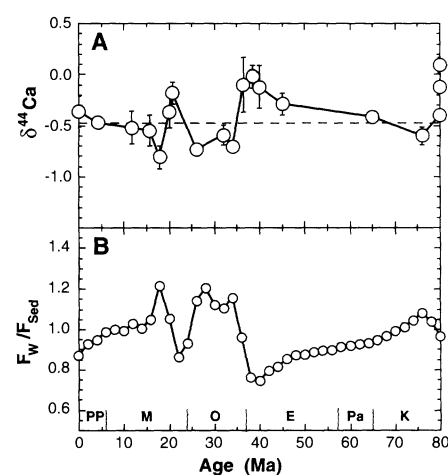


Fig. 1. (A) The $\delta^{44}\text{Ca}$ of marine carbonates over the last 80 Ma. (B) The ratio of the weathering flux of Ca^{2+} into the ocean to the flux of Ca^{2+} out of the ocean due to sedimentation of carbonates. $F_{\text{W}}/F_{\text{Sed}}$ is calculated from Eq. 5 with $\delta_{\text{SW}} = \delta_{\text{sed}} - \Delta_{\text{Sed}}$, by using a 30-term Fourier fit to the data in (A) for δ_{sed} , $\Delta_{\text{Sed}} = -0.5\text{‰}$, and $\delta_{\text{W}} = -0.5\text{‰}$.

¹Berkeley Center for Isotope Geochemistry, Department of Geology and Geophysics, University of California, Berkeley, CA 94720–4767, USA. ²Earth Sciences Division, E. O. Lawrence Berkeley National Laboratory, Berkeley, CA 94720, USA.

*Present address: Department of Earth Sciences, University of Cambridge, Downing Street, Cambridge CB2 3EQ, UK.

of our estimates for $\delta^{44}\text{Ca}$ of the weathering fluxes (-0.44%) and Δ_{Sed} (-1.3%), the predicted steady-state value for seawater Ca^{2+} is $+0.86\%$, which matches the measured value (Table 1). From our analysis it therefore appears that the present-day system is close to steady state (30). Zhu and Macdougall (12) argue that the system is not in steady state on the basis of their analyses of deep-sea carbonates that imply a Δ_{Sed} of -2.1% , and therefore a steady-state seawater $\delta^{44}\text{Ca}$ value of $+1.8\%$. However, the -2.1% value for Δ_{Sed} does not appear to be consistent with the bulk of existing data.

The expected magnitude of variations in the $\delta^{44}\text{Ca}$ of seawater Ca^{2+} can be estimated by rewriting Eq. 1 with the weathering fluxes grouped together:

$$\frac{N_{\text{Ca}} d\delta_{\text{sw}}}{dt} = F_{\text{w}}(\delta_{\text{w}} - \delta_{\text{sw}}) - F_{\text{Sed}}\Delta_{\text{Sed}} \quad (3)$$

If the weathering and sedimentary fluxes are unequal for any period longer than τ_{Ca} , the $\delta^{44}\text{Ca}$ of seawater will reach a quasi-steady state value that reflects this imbalance, whereas seawater concentrations of Ca^{2+} will continue to change. Roughly, the left side of Eq. 3 can be set to zero to obtain

$$\delta_{\text{sw}}(t) \approx \delta_{\text{w}}(t) - \frac{F_{\text{Sed}}}{F_{\text{w}}}(t)\Delta_{\text{Sed}} \quad (4)$$

and

$$\delta_{\text{Sed}}(t) \approx \delta_{\text{w}}(t) - \Delta_{\text{Sed}} \left[\frac{F_{\text{Sed}}(t)}{F_{\text{w}}} - 1 \right] \quad (5)$$

Equation 4 gives the seawater $\delta^{44}\text{Ca}$ value, whereas Eq. 5 gives the $\delta^{44}\text{Ca}$ value of ma-

rine biogenic carbonate and applies to the data in Fig. 1A.

Variations in the $\delta^{44}\text{Ca}$ of seawater reflect variations in Δ_{Sed} and/or δ_{w} , or inequality of F_{Sed} and F_{w} . δ_{w} may shift if the ratio of silicate to carbonate weathering changes. The $\delta^{44}\text{Ca}$ difference between silicates and carbonates of about 0.4% limit δ_{w} variations to about 0.2% . For a flux imbalance, if sedimentation is greater than input ($F_{\text{Sed}} > F_{\text{w}}$), the $\delta^{44}\text{Ca}$ of seawater should increase and the seawater Ca^{2+} concentrations should decrease, and vice versa. Assuming that the ratio $F_{\text{Sed}}/F_{\text{w}}$ varies from roughly 0.7 to 1.3 (2, 3), then the seawater variations in $\delta^{44}\text{Ca}$ could span a range of about $0.6\Delta_{\text{Sed}}$ or 0.8% . Changes of Δ_{Sed} do not affect the carbonate record unless there are also changes in the ratio $F_{\text{Sed}}/F_{\text{w}}$.

The $\delta^{44}\text{Ca}$ range measured on carbonate sediments of Cretaceous and younger age is 0.9% (Fig. 1A). This range is too large to be caused solely by changes in δ_{w} , but is approximately the correct magnitude for variations caused by imbalances between weathering and sedimentation fluxes. The features that we consider significant are the relatively high $\delta^{44}\text{Ca}$ values in the late Eocene [46 to 36 million years ago (Ma)] and early Miocene (22 to 20 Ma), and the relatively low $\delta^{44}\text{Ca}$ values in the Oligocene (34 to 26 Ma) and middle Miocene (18 to 14 Ma). A low $\delta^{44}\text{Ca}$ corresponds to periods where weathering input of Ca^{2+} exceeds sedimentary output (Fig. 1B).

A relatively large Ca^{2+} weathering flux might be expected for the Oligocene and middle Miocene periods, for which there is evidence for rapid erosion of the Himalaya (14, 31–34) and a rapid rise in seawater $^{87}\text{Sr}/^{86}\text{Sr}$ ratios (14–18). The Sr signal is heavily influenced by the radiogenic nature of the silicate weathering products in the Himalaya, but the Ca^{2+} signal is not so affected because the Ca^{2+} budget is more heavily weighted toward carbonate weathering. The high $\delta^{44}\text{Ca}$ of the early Miocene samples is interesting because it corresponds with a period of less rapid increase in the seawater Sr isotope ratio. Similarly, the high $\delta^{44}\text{Ca}$ values for the Eocene correspond to a steady or slowly decreasing Sr isotope ratio.

The two periods where $\delta^{44}\text{Ca}$ declines rapidly, at about 36 and 18 Ma, correlate with times of rapid increase in the oxygen isotopic

signature ($\delta^{18}\text{O}$) of benthic foraminifera (19), which is indicative of an increase in the size of polar and continental ice sheets and hence of a drop in ocean temperature. Thus, low $\delta^{44}\text{Ca}$ correlates with global cooling. Expansion of ice sheets and the concomitant drop in sea level also expose wide continental platforms to erosion, which should result in an increased weathering flux of Ca^{2+} to the ocean, largely from older carbonate rocks.

The observation that periods of low $\delta^{44}\text{Ca}$ correspond to periods of lower global temperature suggests that, during times of low global temperature, there is an increasing $[\text{Ca}^{2+}]$ in the oceans. Assuming that the oceans are maintained approximately at calcite saturation (2, 3), an increase in $[\text{Ca}^{2+}]$ could be accommodated with a proportionate decrease in $[\text{HCO}_3^-]$ and atmospheric CO_2 if pH is independently buffered (35). For an end-member model of constant pH, atmospheric P_{CO_2} is inversely proportional to $[\text{Ca}^{2+}]$.

With sufficient Ca^{2+} isotopic data it is possible to calculate the marine $[\text{Ca}^{2+}]$ back through geologic time, starting at the present, and therefore estimate atmospheric CO_2 concentrations through time for different paleo-pH scenarios. To do this effectively requires Ca^{2+} isotopic data at time intervals spaced at significantly less than the 1-million-year residence time of Ca^{2+} in the ocean, and hence cannot yet be done. However, our modeling of the sparse data of Fig. 1A suggests that, for a reasonable range of assumed values for δ_{w} and Δ_{Sed} , Ca^{2+} has been generally increasing over the past 35 to 40 Ma. For the case of constant pH or for increasing pH over this time interval, the change in Ca^{2+} corresponds to decreasing atmospheric P_{CO_2} , matching trends in other reconstructions (36).

References and Notes

1. C. Urey, *The Planets, Their Origins and Development* (Yale Univ. Press, New Haven, CT, 1952).
2. R. A. Berner, A. C. Lasaga, R. M. Garrels, *Am. J. Sci.* **283**, 641 (1983).
3. A. C. Lasaga, R. A. Berner, R. M. Garrels, in *The Carbon Cycle and Atmospheric CO_2 . Natural Variations Archean to Present*, E. T. Sundquist and W. S. Broecker, Eds. (American Geophysical Union, Washington, DC, 1985), pp. 397–411.
4. M. E. Raymo, W. F. Ruddiman, P. N. Froelich, *Geology* **16**, 649 (1988).
5. W. S. Broecker and T.-H. Peng, *Tracers in the Sea* (Eldigio Press, Palisades, NY, 1982).
6. S. Kempe and E. T. Degens, *Chem. Geol.* **53**, 95 (1985).
7. B. H. Wilkinson and R. K. Given, *J. Geol.* **94**, 321 (1986).
8. B. H. Wilkinson and T. J. Algeo, *Am. J. Sci.* **289**, 1158 (1989).
9. R. J. Spencer and L. A. Hardie, in *Fluid-Mineral Interactions: A Tribute to H. P. Eugster*, R. J. Spencer and I.-Ming Chou, Eds. (Geochemical Society, San Antonio, TX, 1990), pp. 409–419.
10. S. M. Stanley and L. A. Hardie, *Palaeogeogr. Palaeoclimatol. Palaeoecol.* **107**, 243 (1998).
11. There are six stable isotopes of calcium: ^{40}Ca , ^{42}Ca , ^{43}Ca , ^{44}Ca , ^{46}Ca , and ^{48}Ca . Variations in the relative abundance of these isotopes is expressed as a delta value: $\delta^{44}\text{Ca} = [({}^{44}\text{Ca}/{}^{40}\text{Ca})_{\text{sample}}/({}^{44}\text{Ca}/{}^{40}\text{Ca})_{\text{standard}} - 1]$.

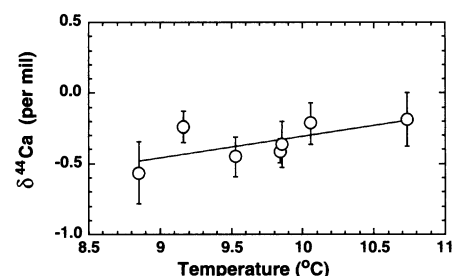


Fig. 2. $\delta^{44}\text{Ca}$ versus growth temperature in the temperate intertidal foraminifera, *Glabratella ornata*. The line shown is $\delta^{44}\text{Ca} = 0.1537 - 1.838T$, $r^2 = 0.45$.

Table 1. Calcium isotopic composition of seawater Ca^{2+} .

Location	Latitude and longitude	Depth (m)	$\delta^{44}\text{Ca}^*$ (‰)
Sargasso Sea†	31°40'N, 64°10'W	300	0.80 ± 0.19
Subantarctic Atlantic	46°57'S, 6°15'E	4066	0.86 ± 0.21
Santa Barbara Basin	34°15'N, 119°55'W	0	0.87 ± 0.26
San Diego†	32°52'N, 117°16'W	0	0.92 ± 0.18
Central North Pacific	31°28'N, 136°6'W	500	0.85 ± 0.09

* $\delta^{44}\text{Ca}$ and $\pm 2\sigma$ values are based on two to three separate measurements. †Bermuda Atlantic Time-Series site (BATS). ‡Data from Skulan et al. (27).

- $1] \times 10^3$, where the standard, described in (27), is an ultrapure sample of CaCO_3 .
12. P. Zhu and J. D. MacDougall, *Geochim. Cosmochim. Acta* **62**, 1691 (1998).
 13. The procedures for the chemical separation and mass spectrometric analysis of calcium are modified from those described in Russell *et al.* (37) and Marshall and DePaolo (38) and are described by Skulan *et al.* (27). A mixed ^{42}Ca - ^{48}Ca tracer is added to carbonate samples that have been dissolved in HCl or is added directly to seawater samples. With the seawater samples, the sample-tracer mixture is loaded onto a cation-exchange column packed with Dowex resin and eluted with HCl. Calcium is then loaded onto Ta filaments for mass spectrometric analysis on a VG Sector 54E modified to have one large bucket Faraday collector. Using three ratios, $^{42}\text{Ca}/^{40}\text{Ca}$, $^{44}\text{Ca}/^{40}\text{Ca}$, and $^{48}\text{Ca}/^{40}\text{Ca}$, we solve for three unknowns: the tracer/sample ratio, the mass discrimination, and the sample $^{44}\text{Ca}/^{40}\text{Ca}$ ratio. Solution of the equations is done iteratively.
 14. C. H. Chen, D. J. DePaolo, C.-Y. Lan, *Earth Planet. Sci. Lett.* **143**, 125 (1996).
 15. D. J. DePaolo and K. L. Finger, *Geol. Soc. Am. Bull.* **103**, 112 (1991).
 16. F. M. Richter, D. B. Rowley, D. J. DePaolo, *Earth Planet. Sci. Lett.* **109**, 11 (1992).
 17. D. A. Hodell and F. Woodruff, *Paleoceanography* **9**, 405 (1994).
 18. J. S. Oslick, K. G. Miller, M. D. Feigenson, J. D. Wright, *Paleoceanography* **9**, 427 (1994).
 19. K. G. Miller, R. G. Fairbanks, G. S. Mountain, *Paleoceanography* **2**, 1 (1987).
 20. J. M. Gieskes and J. R. Lawrence, *Geochim. Cosmochim. Acta* **45**, 1687 (1981).
 21. H. Elderfield and A. Schultz, *Annu. Rev. Earth Planet. Sci.* **24**, 191 (1996).
 22. The dominant input of Ca^{2+} to the ocean comes from rivers, with 1.2×10^{13} to 1.5×10^{13} mol year^{-1} being the current estimate (39, 40). The major output of Ca^{2+} occurs as the deposition of carbonate sediments on the seafloor, presently estimated at 2.9×10^{13} mol year^{-1} (41).
 23. M. G. Erskine and J. H. Lipps, *J. Foraminiferal Res.* **17**, 240 (1987).
 24. *Emiliania huxleyi* isolate CCMP 1742 (Provasoli-Guillard National Center for Culture of Marine Phytoplankton) was grown under cool white lights, on a 14–10 hour light-dark cycle at 16°C in f/2-Si media (42).
 25. J. Skulan and D. J. DePaolo, *Proc. Natl. Acad. Sci. U.S.A.* **96**, 13709 (1999).
 26. Examples of wider variability (fractionations of –0.47 and –0.88‰ relative to seawater) are provided by tests of the tropical foraminifera, *Alveolinella quoyi* and *Marginopora vertebralis* (23). Both *A. quoyi* and *M. vertebralis* are unusually large foraminifera (with diameters up to 12 and 30 mm, respectively) and harbor photosynthetic symbionts (43, 44). Both of these features may affect Ca^{2+} uptake and mineralization rates and thus potentially alter Ca^{2+} isotopic fractionation.
 27. J. Skulan, D. J. DePaolo, T. L. Owens, *Geochim. Cosmochim. Acta* **61**, 2505 (1997).
 28. Values for the Ca^{2+} isotopic composition of rivers reported by Zhu and MacDougall (12) were normalized to our standard, purified CaCO_3 (27) with seawater (the only material common to both studies) as an anchor point. The isotopic value of the rivers relative to the CaCO_3 standard ($\delta^{44}\text{Ca}_{\text{CCstd}}$) are equal to the isotopic difference between the rivers and seawater measured with the old standard minus the difference between the CaCO_3 standard and seawater relative to CaCO_3 : $\delta^{44}\text{Ca}_{\text{riverCCstd}} = (\delta^{44}\text{Ca}_{\text{riveroldstd}} - \delta^{44}\text{Ca}_{\text{SWoldstd}}) - (\delta^{44}\text{Ca}_{\text{CCstd}} - \delta^{44}\text{Ca}_{\text{SWCCstd}})$ or $\delta^{44}\text{Ca}_{\text{CCstd}} = (\delta^{44}\text{Ca}_{\text{riveroldstd}} - 0\text{‰}) - (0\text{‰} - 0.9\text{‰})$.
 29. The silicate weathering flux to the oceans may have a $\delta^{44}\text{Ca}$ that is lower than the average $\delta^{44}\text{Ca}$ of igneous rocks if there is fractionation associated with weathering. If so, there is an additional reservoir with relatively high $\delta^{44}\text{Ca}$ composed of silicate weathering residues. Hence, clay-rich sediments and some soils may have significantly elevated $\delta^{44}\text{Ca}$ values.
 30. The modern system is not at steady-state owing to effects related to the last deglaciation (45). However, because the duration of the imbalance is so short (10,000 years) relative to the residence time of Ca^{2+} in seawater, there is no observable $\delta^{44}\text{Ca}$ effect.
 31. R. B. Sorkhabi and E. Stump, *Geol. Soc. Am. Today* **3**, 85 (1993).
 32. T. M. Harrison, P. Copeland, W. S. F. Kidd, A. Yin, *Science* **255**, 1663 (1992).
 33. P. Copeland, T. M. Harrison, W. S. F. Kidd, R. Xu, Y. Zhang, *Earth Planet. Sci. Lett.* **86**, 240 (1987).
 34. S. Guillot, K. Hodges, P. LeFort, A. Pecher, *Geology* **22**, 559 (1994).
 35. The solubility product constant for calcite can be written in the form: $K_{\text{sp}} = [\text{Ca}^{2+}][\text{HCO}_3^-]^2/P_{\text{CO}_2}$. An increase in $[\text{Ca}^{2+}]$ will accompany an increase in P_{CO_2} in the absence of effects from other ions in solution (46). If pH is buffered, an increase in $[\text{Ca}^{2+}]$ would be compensated by a decrease in P_{CO_2} . To fully constrain P_{CO_2} requires an independent measure of pH, such as the boron isotopic composition of foraminifera (47, 48). The temperature dependence of K_{sp} , the concentrations of other ions in seawater, and differences between the surface and deep ocean also come into play.
 36. M. Pagani, K. H. Freeman, M. A. Arthur, *Science* **285**, 876 (1999).
 37. W. A. Russell, D. A. Papanastassiou, T. A. Tombrello, *Geochim. Cosmochim. Acta* **42**, 1075 (1978).
 38. B. D. Marshall and D. J. DePaolo, *Geochim. Cosmochim. Acta* **46**, 2537 (1982).
 39. M. Meybeck, *Rev. Geol. Dyn. Geogr. Phys.* **21**, 215 (1979).
 40. J. D. Milliman, *Global Biogeochem. Cycles* **7**, 927 (1993).
 41. B. N. Opdyke and B. H. Wilkinson, *Paleoceanography* **3**, 685 (1988).
 42. R. R. L. Guillard, in *Culture of Marine Invertebrate Animals*, W. L. Smith and M. H. Chanley, Eds. (Plenum, New York, 1975), pp. 26–60.
 43. J. H. Lipps and K. P. Severin, *Sci. New Guinea* **11**, 126 (1984/85).
 44. Y. Song, R. G. Black, J. H. Lipps, *Paleobiology* **20**, 14 (1994).
 45. E. K. Berner and R. A. Berner, *Global Environment: Water, Air, and Geochemical Cycles* (Prentice-Hall, Upper Saddle River, NJ, 1996).
 46. J. J. Drever, *The Geochemistry of Natural Waters* (Prentice-Hall, Englewood Cliffs, NJ, 1982).
 47. P. N. Pearson and M. R. Palmer, *Science* **284**, 1824 (1999).
 48. A. J. Spivack, C. F. You, H. J. Smith, *Nature* **363**, 149 (1993).
 49. We thank T. Owens, B. L. Ingram, H. Tolliver, E. B. Roark, J. Skulan, J. Lipps, A. Lessen, M. Hendricks, D. Schrag, C. M. Preston, K. Wetmore, P. N. Froelich, the BATS crew, M. H. Garcia, and D. Penry for samples, advice, and assistance, and two anonymous reviewers for helpful comments. Supported by NSF grants EAR9526997 and EAR9909639 (D.J.D.) and by a University of California, Berkeley, Chancellor's Postdoctoral Fellowship (C.L.D.).

5 April 2000; accepted 20 June 2000

Earthquake Potential Along the Northern Hayward Fault, California

Roland Bürgmann,^{1*} D. Schmidt,¹ R. M. Nadeau,¹ M. d'Alessio,¹ E. Fielding,² D. Manaker,³ T. V. McEvilly,¹ M. H. Murray¹

The Hayward fault slips in large earthquakes and by aseismic creep observed along its surface trace. Dislocation models of the surface deformation adjacent to the Hayward fault measured with the global positioning system and interferometric synthetic aperture radar favor creep at ~7 millimeters per year to the bottom of the seismogenic zone along a ~20-kilometer-long northern fault segment. Microearthquakes with the same waveform repeatedly occur at 4- to 10-kilometer depths and indicate deep creep at 5 to 7 millimeters per year. The difference between current creep rates and the long-term slip rate of ~10 millimeters per year can be reconciled in a mechanical model of a freely slipping northern Hayward fault adjacent to the locked 1868 earthquake rupture, which broke the southern 40 to 50 kilometers of the fault. The potential for a major independent earthquake of the northern Hayward fault might be less than previously thought.

On 21 October 1868, the only known historic major earthquake [magnitude (M) ≈ 7] on the Hayward fault ruptured the southern fault segment over a distance of 40 to 50 km from

Fremont to Berkeley (Fig. 1A) (1). Investigations of paleoseismic (2) and historic (3) data suggest that the most recent earthquake north of the 1868 rupture occurred between 1640 and 1776. Long-term slip rate estimates of ~10 mm/year suggest that 2.2 to 3.6 m of seismic slip potential have accumulated since the most recent event on the northern Hayward fault (4, 5). Thus, the Hayward–Rodgers Creek fault zone is commonly assigned the highest earthquake probability of any fault in the San Francisco Bay area (6). However, estimates of elastic strain to be released in future events are complicated by the occurrence of aseis-

¹Department of Earth and Planetary Science and Berkeley Seismological Laboratory, 307 McCone Hall, University of California, Berkeley, Berkeley, CA 94720, USA. ²Mail Stop 300-233, Jet Propulsion Laboratory, California Institute of Technology, 4800 Oak Grove Drive, Pasadena, CA 91109, USA. ³Department of Geology, University of California, Davis, Davis, CA 95616, USA.

*To whom correspondence should be addressed. E-mail: burgmann@seismo.berkeley.edu